

Contrastive Alignment with Semantic Gap-Aware Corrections in Text-Video Retrieval

Jian Xiao Zijie Song Jialong Hu Hao Cheng Zhenzhen Hu* Jia Li*

Richang Hong

School of Computer Science and Information Engineering,
Hefei University of Technology, Hefei, China

{j.xiao_hfut, chenghao}@mail.hfut.edu.cn zjsonghfut@gmail.com
zdszds534@gmail.com {zzhu, lijia}@hfut.edu.cn hongrc.hfut@gmail.com

Abstract

Recent advances in text-video retrieval have been largely driven by contrastive learning frameworks. However, existing methods overlook a key source of optimization tension: the separation between text and video distributions in the representation space—referred to as the modality gap—and the prevalence of false negatives in batch sampling. These factors lead to conflicting gradients under the InfoNCE loss, impeding stable alignment. To mitigate this, we propose GARE—a Gap-Aware Retrieval framework that introduces a learnable, pair-specific increment Δ_{ij} between text t_i and video v_j to offload the tension from the global anchor representation. We first derive the ideal form of Δ_{ij} via a coupling multivariate first-order Taylor approximation of the InfoNCE loss under a trust-region constraint, revealing it as a key mechanism for resolving gradient conflicts by guiding updates along a locally optimal descent direction in the coupled optimization landscape. Due to the expensive cost of directly approximate Δ_{ij} , we introduce a lightweight neural module conditioned on the semantic gap between each video-text pair, enabling structure-aware correction guided by gradient supervision. To further stabilize learning and promote interpretability, we regularize Δ via three components: a trust-region constraint regularization to prevent oscillations, a directional diversity term to expand the semantic difference space, and an information bottleneck over Δ to restrict redundant information. Experiments across four retrieval benchmarks show that GARE consistently improves alignment accuracy and robustness to noisy supervision, confirming the effectiveness of gap-aware tension unloading. Code is available at <https://github.com/musicman217/GARE-text-video-retrieval>.

1 Introduction

Text-video retrieval (TVR) [48] is a fundamental task in video understanding, aiming to retrieve relevant videos given a text query [29, 28, 39, 15]. With the proliferation of short video platforms, this task has attracted growing research interest. In recent years, vision-language pretraining models such as CLIP [33] have shown great success in cross-modal representation alignment, demonstrating strong performance on various retrieval benchmarks. These models typically learn a shared embedding space by aligning visual and textual modalities through large-scale contrastive learning [43, 18, 8, 9, 17, 40, 19, 27], and have thus become a popular backbone in TVR systems.

*Corresponding author.

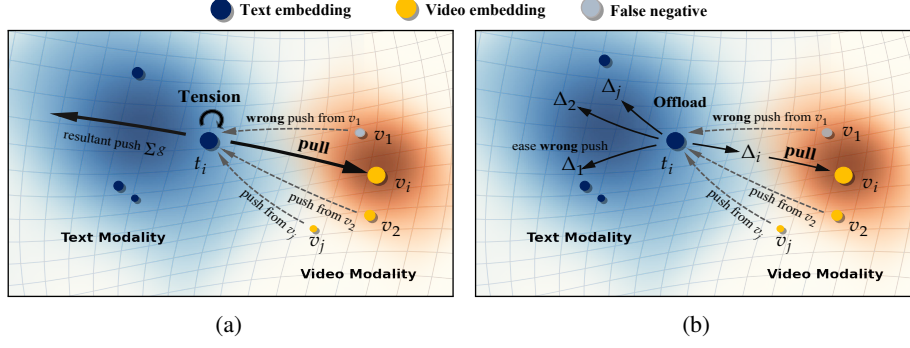


Figure 1: **Tension and false negative challenge vs. our tension offloading strategy.** (a) Due to modality gap [27] and false negatives [38], the gradients from negative samples partially overlap with the correct direction, leading to gradient tension around the anchor t_i . This restricts its optimization freedom and causes erroneous updates. (b) We offload part of the optimization pressure from t_i to the learned increment Δ_{ij} by relaxing the gradient. This relieves gradient tension and reduces the impact of false negatives on t_i , as errors are partially absorbed by Δ . Each Δ_{ij} captures a semantically meaningful correction of the text-video gap.

Despite the empirical success of contrastive learning in text-video retrieval, existing methods largely overlook two fundamental sources of optimization tension. First, the significant modality gap between text and video representations: the two modalities often reside in disjoint regions of the embedding space [27, 47], with markedly different semantic structures and high distributional divergence (e.g., large KL divergence between modality-wise feature distributions). This separation creates an inherent geometric and semantic mismatch that cannot be easily bridged by global metric learning. Second, the prevalence of false negatives: semantically similar but unlabeled text-video pairs—further injects noisy gradient signals during training [10, 7], as they are incorrectly treated as hard negatives. These two factors jointly induce unstable or conflicting optimization forces during contrastive learning, especially under the coupled softmax structure of InfoNCE [32]. Without an explicit mechanism to account for these challenges, models often converge to suboptimal solutions, particularly on semantically ambiguous or structurally complex samples.

Figure 1a provides an overview of the optimization tension caused by modality gaps, where text and video embeddings lie in well-separated regions of the representation space—this repulsion tends to push t_i away from the entire video manifold. As a result, the positive and negative terms impose a conflicting descent direction, both acting along the same region but with opposing effects. This constitutes a core source of optimization tension in contrastive learning. In addition, false negatives—semantically relevant but unlabeled pairs—introduce noisy repulsion that further distorts the optimization trajectory, especially in early training.

To address both issues, we introduce a pair-specific increment Δ_{ij} that acts as a learnable adjustment between t_i and v_j . As shown in Figure 1b, instead of enforcing all semantic correction on the anchor embedding t_i , we allow Δ_{ij} to absorb part of the optimization signal at the pair level. This design serves two complementary purposes: 1) it unloads the global optimization tension caused by the modality gap by decoupling the descent direction across different video-text pairs; 2) it buffers the local gradient noise introduced by false negatives, preventing anchor representations from drifting due to misaligned repulsion.

To ensure that Δ_{ij} contributes constructively to the loss landscape, we derive its ideal form via a first-order Taylor expansion of the contrastive loss under a trust-region constraint. While the exact solution is intractable due to inter-pair coupling, we approximate it using a lightweight neural module that conditions on the semantic gap $v_j - t_i$, allowing the model to proactively infer alignment adjustments before receiving backpropagated signals. This results in a closed-loop training dynamic: the model first estimates a gap-aware correction based on its prior belief, then updates this belief through feedback from contrastive supervision. Together, this enables more stable training and more accurate modeling of semantic structure under noise.

We further analyze the geometric behavior of the learned increment Δ_{ij} . Empirically, we observe that Δ_{ij} tends to form an obtuse angle with the initial gap vector $v_j - t_i$, averaging around 1.6 radians. This indicates that the model is not merely copying the raw modality difference, but is instead learning a structure-aware correction that incorporates higher-level alignment priors. Moreover, we find that the Euclidean distance between paired embeddings increases after applying Δ_{ij} , suggesting that the model leverages pair-level adjustment to release optimization tension and enable finer-grained control over semantic positioning on the unit sphere. Our contributions are as follows:

- We analyze the gradient structure of the InfoNCE loss and reveal its inherent multi-variable coupling behavior via introduced multiple increments Δ . By performing a first-order Taylor expansion under a local trust region, we derive an optimal update rule for each pairwise increment Δ_{ij} that aligns with the descent direction of InfoNCE.
- Building on this formulation, we propose a gap-aware retrieval framework where each increment Δ_{ij} is predicted by a learnable network and directly participates in the forward pass. This design enables explicit offloading of gradient tension from text anchors, thereby mitigating misaligned updates caused by modality gap and false negatives.
- We validate our method on four cross-modal retrieval benchmarks, i.e., MSR-VTT [45], DiDeMo [2], ActivityNet Captions [24], MSVD [6], demonstrating consistent improvements. Further analysis shows that the learned increments are semantically meaningful and geometrically structured, highlighting their role in stable and interpretable optimization.

2 Related work

Contrastive Learning and Modality Gap Contrastive learning has become a foundational paradigm in multimodal representation learning. Wang and Isola [40] formalize contrastive learning via the principles of alignment and uniformity on the hypersphere, offering a geometric perspective on representation quality. Wang and Liu [38] show that contrastive loss is hardness-aware and temperature-sensitive, and reveal a trade-off between representation uniformity and semantic tolerance, highlighting the need to preserve meaningful structure among semantically similar samples. Liang et al. [27] investigate the modality gap in multimodal contrastive learning and attribute it to initialization imbalance and cone effects. False negatives have also been recognized as a key challenge in contrastive learning [10, 7], with solutions ranging from reweighting and elimination to dynamic detection and correction.

Text-Video Retrieval Text-video retrieval is one of the prominent tasks [13, 23, 37, 3, 16, 44, 31, 4, 21, 25, 41] in cross-modal learning. The majority of existing research [26, 14, 22, 30, 42, 5, 46] in this area utilizes a mapping technique that aligns both text and video inputs within a shared latent space to facilitate direct similarity assessment. CLIP4Clip [29] is the first to adapt CLIP [33] for video-text retrieval via temporal frame aggregation. TS2-Net [28] improves temporal modeling through token shift and selection. X-Pool [15] introduces text-guided pooling to highlight salient video tokens. HBI [19] values possible correspondences between frames and words using Banzhaf interaction for sensitive and explainable cross-modal alignment. EMCL [19] introduces an expectation-maximization [11] framework to learn a compact latent space where video and text features are represented as linear combinations of shared bases. This decomposition reduces the rank of the latent space, mitigating the modality gap and enhancing semantic alignment. Unlike prior works that refine matching structures, our method analyzes the gradient form of InfoNCE and introduces a learnable gap-aware increment Δ_{ij} to offload optimization tension, enabling structured optimization in a trust-region-aware formulation.

3 Approach

We propose a gap-aware retrieval framework that introduces a learnable, pair-specific increment Δ_{ij} to adjust text features toward video embeddings or vice versa. To alleviate optimization tension and false negatives, we derive Δ_{ij} via a first-order Taylor expansion of the InfoNCE loss and approximate it using a neural module ψ conditioned on the semantic gap. We further regularize Δ_{ij} in norm, direction, and distribution to enhance its structure and interpretability.

3.1 Preliminaries

Task Definition Given a dataset of N paired video-text examples $\{(v_i, t_i)\}_{i=1}^N$, the goal of text-video retrieval is to learn a pair of encoders: a visual encoder $\phi_v(\cdot)$ and a text encoder $\phi_t(\cdot)$, that map inputs into a shared embedding space. The similarity between any pair (v_j, t_i) is computed using a scoring function, typically the cosine similarity:

$$s_{ij} = \frac{\phi_t(t_i)^\top \phi_v(v_j)}{\|\phi_t(t_i)\| \cdot \|\phi_v(v_j)\|}, \quad (1)$$

where $\phi_t(t_i) \in \mathbb{R}^D$ and D is dimension. During training, contrastive learning is applied to increase the similarity of matched pairs while decreasing that of mismatched ones. At inference, retrieval is performed by ranking all candidate texts (or videos) for a given query video (or text) based on similarity scores. For brevity, we henceforth refer to $\phi_t(t)$ as t , $\phi_v(v)$ as v .

Optimization Tension and First-order Increment Modeling As discussed in the introduction, contrastive optimization in video-text retrieval suffers from gradient tension caused by modality gap and noise from false negatives. These factors hinder stable optimization of the anchor representation t_i , which must simultaneously align with the positive v_i and repel all negatives $v_{j \neq i}$. Formally, the per-anchor InfoNCE loss is given by:

$$\mathcal{L}_i = -\log \frac{e^{\cos(t_i, v_i)/\tau}}{\sum_{j=1}^B e^{\cos(t_i, v_j)/\tau}}, \quad (2)$$

and its gradient with respect to t_i is:

$$\nabla_{t_i} \mathcal{L}_i = \sum_{j=1}^B (p_{ij} - y_{ij}) \cdot \left[\frac{v_j}{\|t_i\| \|v_j\|} - \cos(t_i, v_j) \cdot \frac{t_i}{\|t_i\|^2} \right], \quad (3)$$

where $p_{ij} = \text{softmax}(\cos(t_i, v_j)/\tau)$ and $y_{ij} = \mathbb{1}_{[j=i]}$. As observed in prior works such as [38], the magnitudes of the positive gradient coefficient $|p_{ii} - 1|$ and the aggregate negative terms $\sum_{j \neq i} p_{ij}$ are comparable. In cases of strong modality gap, the attraction from the positive and the repulsion from negatives tend to pull in opposing directions, creating intrinsic gradient tension on t_i .

To alleviate both challenges mentioned above, we introduce a pair-specific increment Δ_{ij} that enables the model to locally adjust the relative positioning between each text-video pair. This increment serves a dual role: it offloads optimization tension by distributing alignment corrections across pairs, and buffers gradient noise by absorbing false-negative interference before it propagates into the anchor embedding. For clarity, we first consider the case where Δ_{ij} is applied to the text side, yielding an adjusted representation:

$$t_{\Delta_{ij}} = t_i + \Delta_{ij}. \quad (4)$$

This formulation allows for certain perturbations at the given anchor t_i corresponding to different v_j respectively. In practice, depending on dataset-specific modality characteristics, the same mechanism can also be applied to the video side (e.g., $v_j + \Delta_{ij}$). However, this flexibility raises a central question: how should each Δ_{ij} be optimized to effectively reduce the contrastive loss?

A naive approach would linearize the loss around the original anchor t_i (i.e., $\Delta_{i*} = 0$), treating each Δ_{ij} as an independent perturbation. However, under this formulation, the gradient $\nabla_{\Delta_{ij}} \mathcal{L}_i$ depends only on the static similarity $\cos(t_i, v_j)$, failing to account for the influence of other Δ_{ik} in the same batch. This leads to decoupled gradients that ignore the softmax coupling intrinsic to InfoNCE. More importantly, expanding the loss only at t_i results in a univariate approximation, which does not reflect how different Δ_{ij} collectively reshape the similarity ranking across all v_j . Since our goal is to adjust the relative structure of the entire pair set for each anchor, we require a multivariate formulation where all Δ_{ij} are coupled and optimized under a shared comparison scale.

To address this, we treat all Δ_{ij} as jointly optimized variables, and reinterpret the per-anchor contrastive loss \mathcal{L}_i as multivariate function over the full set $\{\Delta_{ij}\}_{j=1}^B$:

$$\mathcal{L}_i(\Delta_{i1}, \dots, \Delta_{iB}) = -\log \frac{e^{s_{ii}/\tau}}{\sum_{k=1}^B e^{s_{ik}/\tau}}, \quad s_{ij} = \cos(t_i + \Delta_{ij}, v_j). \quad (5)$$

Unlike standard per-sample optimization, the softmax structure couples all Δ_{ij} , meaning the gradient of any single increment depends on the values of the others. To capture this dependency, we perform a multivariate first-order Taylor expansion around a prior coupled state $\Delta_{i*}^{(0)} = \{\Delta_{ij}^{(0)}\}_{j=1}^B$, where all increments are nonzero. In practice, we treat this prior as the current state at iteration t —i.e., we let $\Delta_{i*}^{(t)} := \Delta_{i*}^{(0)}$ —and analyze the local descent behavior from this reference point. This converts our optimization into an iterative process, where each step refines the current set of coupled increments. The resulting linear approximation is:

$$\mathcal{L}_i(\Delta_{i*}) \approx \mathcal{L}_i(\Delta_{i*}^{(t)}) + \sum_{j=1}^B \left[\nabla_{\Delta_{ij}} \mathcal{L}_i(\Delta_{i*}^{(t)}) \right]^\top (\Delta_{ij} - \Delta_{ij}^{(t)}). \quad (6)$$

Crucially, this expansion preserves the softmax-induced coupling: each gradient term $\nabla_{\Delta_{ij}} \mathcal{L}_i$ is evaluated assuming that all other increments $\Delta_{ik \neq j}$ remain fixed at their nonzero states. The resulting linearized loss defines a local descent landscape for each Δ_{ij} . To ensure reliable updates within this approximation, we impose a trust-region constraint that bounds the update magnitude:

$$\|\Delta_{ij}\| \leq \varepsilon, \quad (7)$$

which reflects our belief that meaningful corrections should occur within a localized region around t_i . Under this constraint, the optimal update direction for each Δ_{ij} corresponds to steepest descent along its local gradient:

$$\Delta_{ij}^{*(t+1)} = \Delta_{ij}^{(t)} - \alpha_{ij}^{(t)} \cdot \frac{\nabla_{\Delta_{ij}} \mathcal{L}_i(\Delta_{i*}^{(t)})}{\|\nabla_{\Delta_{ij}} \mathcal{L}_i(\Delta_{i*}^{(t)})\|}, \quad (8)$$

where step size $\alpha_{ij}^{(t)}$ is analytically determined to ensure $\|\Delta_{ij}^{(t+1)}\| \leq \varepsilon$ and derived via the Cauchy–Schwarz inequality to project onto the trust-region boundary (see Appendix D for details). This yields the steepest descent direction of the linearized loss, evaluated at a coupled batch state $\Delta_{i*}^{(t)}$, where all increments are fixed but nonzero. While conceptually similar to coordinate-wise proximal optimization, directly applying this solution is impractical due to two key challenges: 1) gradient coupling: each $\nabla_{\Delta_{ij}} \mathcal{L}_i$ depends on all other Δ_{ik} , making updates interdependent and unstable; 2) scale ambiguity: the optimal trust-region radius ε may vary across pairs depending on semantic difficulty or training stage. To address this, we adopt a learnable network that directly predicts the coupled increment state $\Delta_{i*}^{(t)}$ based on the semantic gap $v_j - t_i$. The subsequent update to $\Delta_{i*}^{(t+1)}$ is implicitly performed via backpropagation on the InfoNCE loss. Since the gradient of the loss naturally aligns with the steepest descent direction, this formulation allows us to transform the iterative update rule into a trainable network prediction problem, enabling amortized, structure-aware optimization over the full batch of pairwise increments.

3.2 Gap-Aware Increment Modeling via Pair-Specific Δ_{ij}

To make this optimization tractable, we replace the explicit iterative updates with a learnable function ψ that directly predicts each increment $\Delta_{ij}^{(t)}$. Specifically, we amortize the descent process by training a parameterized network ψ to generate the current coupled increment state based on a pairwise semantic difference and a modality-dependent context:

$$\Delta_{ij}^{(t)} = \psi \left(\eta(v_j - t_i), c; \Theta^{(t)} \right), \quad (9)$$

where $\eta \in \{-1, +1\}$ determines the direction of the semantic gap depending on which modality receives the increment. The function ψ is implemented as a single-layer cross-attention module, where the semantic difference $\eta(v_j - t_i)$ serves as the query, and the context vector c —defined based on dataset characteristics—is used as both the key and the value. This allows ψ to generate

Δ_{ij} in a modality- and structure-aware manner, conditioned on the local pairwise discrepancy and auxiliary context. Rather than computing explicit gradient steps, ψ learns to output increments that implicitly reflect the local descent direction. Since Δ_{ij} is embedded directly in the InfoNCE loss, the network is trained end-to-end via backpropagation, allowing it to align its output with the true coupled gradient field. As a result, ψ captures both structure-aware priors and semantic context, producing informed corrections that reduce optimization tension and improve alignment robustness across diverse retrieval scenarios. We now consider the case where $c = v_j$ and the increment Δ_{ij} is added to the text side. In this setting, the two variables t_i and Δ_{ij} share the same gradient flow:

$$\nabla_{t_i} \mathcal{L}_i = \sum_{j=1}^B \nabla_{t_{\Delta_{ij}}} \mathcal{L}_i, \quad \nabla_{\Delta_{ij}} \mathcal{L}_i = \nabla_{t_{\Delta_{ij}}} \mathcal{L}_i, \quad (10)$$

where the gradient with respect to each perturbed anchor is given by:

$$\nabla_{t_{\Delta_{ij}}} \mathcal{L}_i = (p_{ij} - y_{ij}) \cdot \left[\frac{v_j}{\|t_{\Delta_{ij}}\| \cdot \|v_j\|} - \cos(t_{\Delta_{ij}}, v_j) \cdot \frac{t_{\Delta_{ij}}}{\|t_{\Delta_{ij}}\|^2} \right]. \quad (11)$$

This formulation introduces a gradient redistribution effect: unlike standard InfoNCE where all gradients act directly on the shared anchor t_i , our pair-specific design allows each negative video v_j to influence only its associated increment Δ_{ij} . The positive pair (t_i, v_i) contributes attraction gradients to both t_i and Δ_{ii} , facilitating alignment; meanwhile, each negative pair (t_i, v_j) , $j \neq i$, applies repulsion primarily to Δ_{ij} . This leads to two key benefits: 1) tension relief — Δ_{ii} can absorb the alignment shift toward v_i , reducing the burden on t_i to resolve large modality gaps in a single step; 2) false-negative suppression — repulsion from semantically similar negatives is redirected into their respective increments, preserving the semantic stability of the anchor representation. We apply this strategy under a symmetric InfoNCE loss:

$$\mathcal{L}_{\text{info}} = -\frac{1}{2} \left(\frac{1}{B} \sum_{i=1}^B \log \frac{e^{s_{ii}/\tau}}{\sum_{j=1}^B e^{s_{ij}/\tau}} + \frac{1}{B} \sum_{j=1}^B \log \frac{e^{s_{ji}/\tau}}{\sum_{i=1}^B e^{s_{ij}/\tau}} \right), \quad (12)$$

This loss function maximizes the similarity of positive pairs $s(t_i + \Delta_{ii}, v_i)$ and minimizes the similarity of negative pairs.

Norm-Based Regularization of Trust-Region Radii Each pair-specific increment Δ_{ij} , predicted by the network ψ , approximates the optimal update direction under the first-order Taylor approximation. Its norm $\varepsilon_{ij} = \|\Delta_{ij}\|_2$ thus serves as a learned trust-region radius, regulating the extent of deviation that t_i can take—regardless of direction—in order to absorb local alignment tension and semantic adjustment. To encourage structure in these radii, we regularize the intra-anchor variance of ε_{ij} across each text anchor. Intuitively, semantically close pairs should have smaller ε_{ij} , while hard negatives benefit from larger ones—yet such structure must be inferred implicitly. We therefore promote norm diversity by minimizing the expected negative variance across anchors:

$$\mathcal{L}_\varepsilon = \mathbb{E}_{t_i \sim \mathcal{B}_t} \left[-\text{Var}(\{\varepsilon_{ij}\}_{j=1}^B) \right], \quad (13)$$

where \mathcal{B}_t denotes the batch of text anchors. This encourages sharper separation between low-confidence and high-confidence pairs, without relying on external supervision. To prevent instability, we apply a lower bound:

$$\mathcal{L}_\varepsilon = \max(\mathcal{L}_\varepsilon, -\lambda), \quad \lambda > 0. \quad (14)$$

This simple yet effective regularization sharpens the implicit trust-region structure learned by ψ , guiding Δ_{ij} to reflect per-pair semantic variability while maintaining stable training dynamics. In the following section, we further complement this with a directional diversity loss to explicitly enhance the angular resolution of Δ_{ij} under each anchor.

Directional Diversity Regularization To enhance the expressiveness of the learned increments Δ_{ij} , we introduce a directional regularization that encourages the directions of $\{\Delta_{ij}\}_{j=1}^B$ under each anchor t_i to be diverse. This helps the model assign distinct update directions to different candidate videos, improving representational resolution and mitigating mode collapse.

We normalize each increment to obtain unit vectors $z_{ij} = \frac{\Delta_{ij}}{\|\Delta_{ij}\|_2}$ and define the regularization loss as the expected angular similarity across all anchor-specific direction sets:

$$\mathcal{L}_{\text{dir}} = \mathbb{E}_{t_i \sim \mathcal{B}_t} [\log \mathbb{E}_{j,k} [\exp(-\sigma \cdot (1 - \langle z_{ij}, z_{ik} \rangle))]] , \quad (15)$$

where σ is a scale factor to control uniformity. This loss softly penalizes directional concentration, while still allowing nearby directions for semantically similar negatives—preserving flexibility under uncertainty. Combined with the norm-based regularization in Section 3.2.1, this term enables fine-grained control over both the magnitude and direction of each increment Δ_{ij} , leading to more stable and structure-aware optimization.

KL Regularization via Information Bottleneck To regularize the distribution of increments Δ_{ij} across text inputs for each video anchor v_j , we introduce a Information Bottleneck (IB) [1, 35] via a KL divergence loss that aligns the empirical distribution with a standard normal prior:

$$\mathcal{L}_{\text{IB}} = \mathbb{E}_{v_j \sim \mathcal{B}_v} [\text{KL}(\mathcal{N}(\mu_j, \sigma_j^2) \parallel \mathcal{N}(0, I))] , \quad (16)$$

where μ_j and σ_j^2 are the mean and variance of $\{\Delta_{ij}\}_{i=1}^B$ over the text batch for each v_j . This loss can be interpreted through the lens of the Information Bottleneck principle: it encourages Δ to retain minimal information about v_j beyond what is necessary for pairwise alignment. By bounding the mutual information $I(\Delta; v_j)$, the model avoids encoding redundant video-specific patterns in Δ . This regularization complements the norm and direction constraints by promoting centered, isotropic, and information-efficient corrections, further enhancing generalization and stability.

Although the input configuration of ψ may vary across datasets, we consistently apply the KL regularization along the video dimension, as video-side representations typically exhibit higher redundancy and local similarity. Regularizing the set of increments associated with each video anchor helps suppress noise and stabilizes learning by enforcing consistent structure across semantically similar pairs. See Appendix.B for an ablation study.

4 Experiment

Datasets, Metrics and Implementation Details *Datasets.* We evaluate our method on four standard text-video retrieval benchmarks: MSR-VTT [45], DiDeMo [2], MSVD [6], and ActivityNet Captions [24]. MSR-VTT contains 10K videos with 20 captions each; we follow the 1K-A test split. DiDeMo includes 10K videos segmented into 5-second clips, each annotated with multiple sentences. MSVD consists of 1.9K short video clips with English captions. ActivityNet Captions provides dense annotations for 20K long-form videos with multiple temporally grounded descriptions.

Metrics. We choose Recall at rank $K=\{1, 5, 10\}$ (R@K), Median Rank (MdR), and mean rank (MnR) to evaluate the retrieval performance.

Implementation Details. We adopt CLIP (ViT-B/32) [33] as the base bi-encoder, equipped with a 4-layer Temporal Transformer [36] for video encoding. Following prior works [29, 15, 26, 39], we use 32-word captions and 12 video frames for MSR-VTT and MSVD, and 64-word captions with 64 frames for DiDeMo and ActivityNet Captions due to their longer video durations. We use the Adam optimizer [12] with linear warm-up, as in prior works. The learning rate is set to $1e-7$ for CLIP’s text and visual encoders, and $1e-4$ for all other modules (except $3e-4$ for ActivityNet). We set $\tau = 0.01$, $\sigma = 2$, and $\lambda = 0.5$. All experiments use a batch size of 128. We train the model for 5 epochs on MSR-VTT, MSVD, and DiDeMo, and 10 epochs on ActivityNet Captions. All experiments are conducted on 4 to 8 GPUs including RTX 4090, A100 and V100.

Comparison with Other Methods Table 1 and Table 2 shows the performance of our method across four standard text-video retrieval benchmarks. As seen, our approach consistently outperforms

Table 1: Comparison results on MSRVT dataset on Text-to-Video Retrieval and Video-to-Text Retrieval.

Methods	Text-to-Video Retrieval					Video-to-Text Retrieval				
	R@1↑	R@5↑	R@10↑	MdR↓	MnR↓	R@1↑	R@5↑	R@10↑	MdR↓	MnR↓
CLIP4Clip [29]	44.5	71.4	81.6	2.0	15.3	42.7	70.9	80.6	2.0	11.6
X-Pool [15]	46.9	72.8	82.2	2.0	14.3	44.4	73.3	84.0	2.0	9.0
TS2-Net [28]	47.0	74.5	83.8	2.0	13.0	45.3	74.1	83.7	2.0	9.2
EMCL-Net [19]	46.8	73.1	83.1	2.0	12.8	46.5	73.5	83.5	2.0	8.8
UATVR [14]	47.5	73.9	83.5	2.0	12.3	46.9	73.8	83.8	2.0	8.6
ProST [26]	48.2	74.6	83.4	2.0	12.4	46.3	74.2	83.2	2.0	8.7
HBI [20]	48.6	74.6	83.4	2.0	12.0	46.8	74.3	84.3	2.0	8.9
Diffusion [22]	49.0	75.2	82.7	2.0	12.1	47.7	73.8	84.5	2.0	8.8
EERCF [34]	47.8	74.1	84.1	-	-	44.7	74.2	83.9	-	-
MPT [49]	48.3	72.0	81.7	-	14.9	46.5	74.1	82.6	-	11.8
Baseline	46.6	73.4	82.2	2.0	12.6	45.6	73.4	82.4	2.0	9.6
GARE (Ours)	49.1	74.7	83.6	2.0	12.0	48.6	75.3	85.3	2.0	8.5

Table 2: Comparison results on DiDeMo, ActivityNet Captions, and MSVD datasets on Text-to-Video Retrieval.

DiDeMo					ActivityNet Captions					MSVD				
Methods	R@1	R@5	R@10	MnR	Methods	R@1	R@5	R@10	MnR	Methods	R@1	R@5	R@10	MnR
TS2-Net	41.8	71.6	82.0	14.8	CLIP4Clip	40.5	72.4	83.6	7.5	CLIP4Clip	45.2	75.5	84.3	10.3
CLIP4Clip	42.8	68.5	79.2	18.9	TS2-Net	41.0	73.6	84.5	8.4	EMCL-Net	42.1	71.3	81.1	17.6
Diffusion	46.7	74.7	<u>82.7</u>	14.3	MPT	41.4	70.9	82.9	7.8	UATVR	46.0	76.3	85.1	<u>10.4</u>
HBI	<u>46.9</u>	<u>74.9</u>	<u>82.7</u>	<u>12.1</u>	HBI	<u>42.2</u>	73.0	<u>84.6</u>	6.6	Diffusion	46.6	75.9	84.1	15.7
Baseline	45.4	74.3	82.0	12.3	Baseline	40.2	72.5	83.6	7.5	Baseline	45.0	75.5	84.5	10.7
GARE (Ours)	47.6	75.4	83.1	12.0	GARE (Ours)	42.6	<u>73.2</u>	84.8	6.6	GARE (Ours)	<u>46.4</u>	<u>76.1</u>	<u>84.5</u>	10.6

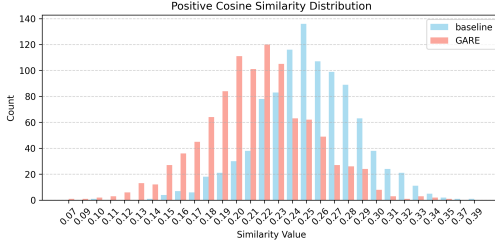
recent state-of-the-art methods on MSR-VTT, ActivityNet and DiDeMo, and a comparable results in MSVD.

Ablative Analysis *Losses design.* We conduct ablation studies on the MSR-VTT 1k-A test set to assess the effectiveness of the proposed increment Δ and its associated regularizers. As shown in the right of Table 3, directly injecting Δ into the InfoNCE flow improves performance from 46.6 to 47.4, validating the benefit of gradient tension release via pairwise adjustment. Introducing the information bottleneck (IB) loss further boosts performance to 48.3, highlighting its role in guiding Δ toward semantically meaningful corrections. However, adding the norm constraint or directional diversity loss alone yields no gain. Notably, combining IB with both the norm and diversity regularizers leads to a substantial improvement, reaching 49.1. This suggests that controlling the update scale (via trust-region) and promoting directional diversity must work together to fully exploit the potential of Δ . This aligns with our design intuition: the trust-region constraint controls the update scale (via ε) but does not regulate directionality, which can lead to redundant or entangled corrections. The diversity regularization ensures that increments associated with the same anchor are directionally distinct, encouraging more uniform and structured behavior around each anchor.

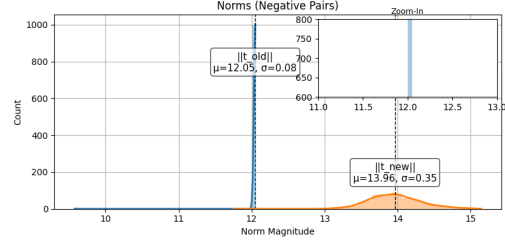
Context Modality Choice in ψ . We evaluate the effect of applying Δ_{ij} to either modality across datasets with contrasting characteristics. As shown in the left of Table 3, on MSR-VTT, injecting Δ on the text side ($t_i + \Delta_{ij}$) achieves the best performance, while applying it to the video side degrades results (R@1 drops to 47.4). This aligns with the fact that MSR-VTT contains many visually similar short clips, making it more effective to adjust the abstract text representation for fine-grained distinctions. Conversely, on ActivityNet, applying Δ to the video side leads to a notable performance boost, whereas modifying text harms results (R@1 \approx 40). This is likely because the long but redundant videos are paired with rich, structured captions—making video-side adaptation more beneficial. These trends highlight the importance of aligning ψ ’s modality choice with dataset structure. For DiDeMo, given its moderate video length (30s), we treat video as the anchor and set $c = v_j$ accordingly.

Table 3: Ablation Studies on Modality Choice and Loss Combinations. *left*: We perform Text-to-Video Task on three datasets on different context modality type of our module ψ . *right*: We perform Text-to-Video Task on MSR-VTT for all losses ablation. First row refers to our baseline.

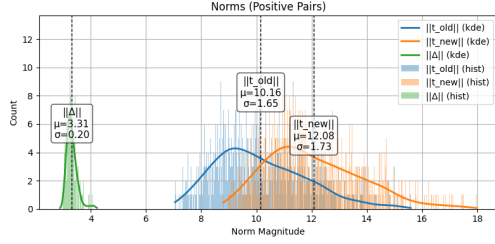
Context Modality Choice of ψ						Losses Ablation							
Modality	Dataset	R@1 \uparrow	R@5 \uparrow	R@10 \uparrow	MnR \downarrow	Δ	\mathcal{L}_{IB}	$\mathcal{L}_{\varepsilon}$	\mathcal{L}_{dir}	R@1 \uparrow	R@5 \uparrow	R@10 \uparrow	MnR \downarrow
$c = t_i$	MSRVTT	47.4	73.5	82.1	12.9					46.6	73.4	82.2	12.6
$c = v_j$	MSRVTT	49.1	73.3	82.2	12.4	✓				47.4	73.8	82.8	12.4
$c = t_i$	ActivityNet	42.6	73.6	84.4	6.8	✓				47.2	73.3	82.2	12.4
$c = v_j$	ActivityNet	40.2	72.2	83.6	8.1	✓			✓	47.0	73.1	82.3	12.6
$c = t_i$	DiDeMo	46.5	74.3	82.6	12.3	✓		✓	✓	47.4	73.7	82.8	12.3
$c = v_j$	DiDeMo	47.6	75.4	83.1	12.0	✓	✓			48.3	74.2	83.2	12.4
						✓	✓	✓	✓	49.1	74.7	83.6	12.0



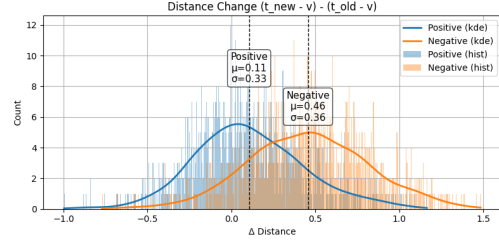
(a) Cosine similarity distribution of positive pairs.



(b) Norm distribution on negative pairs.



(c) Norms distribution on positive pairs.



(d) Distance shift: t_Δ vs. t .

Figure 2: Qualitative analysis on the MSR-VTT 1k-A validation set. t_{new} denotes t_Δ . Our method induces greater angular separation between positive pairs (a), redistributes t_Δ norms to release gradient tension (b, c), and pushes t_Δ outward from v_j (d), promoting uniformity.

More ablation analysis including the lower bound λ of \mathcal{L}_ε , the combination between context modality type c of ψ and η , the scale factor σ of \mathcal{L}_{dir} and the choice of anchor of \mathcal{L}_{IB} can be found in Appendix B.

5 Qualitative Analysis

To understand the effect of the learned increment Δ , we conduct a qualitative analysis on the MSR-VTT 1k-A validation set, focusing on its impact on representation geometry and alignment behavior at inference. As shown in Figure 2a, our method GARE yields lower cosine similarities between positive pairs than the baseline, indicating larger angular separation and improved uniformity on the unit hypersphere [40]. Figures 2b and 2c further show that while t_i is concentrated around norm 12, the offset $t_{\Delta ij}$ exhibits greater and more diverse magnitudes. This supports our view that Δ serves as a tension offloading mechanism, allowing t_i to remain a stable prototype while $t_{\Delta ij}$ absorbs pair-specific adjustments—particularly useful under gradient noise from false negatives. As shown in Figure 2d, $t_{\Delta ij}$ is generally farther from v_j than t_i , indicating that the model does not simply pull pairs closer but expands the representation scale to allow more flexible alignment. This explains why, despite lower cosine similarity, GARE achieves better uniformity and geometric balance. Additional training-time analysis is provided in Appendix C.

6 Conclusion

This paper investigates the optimization behavior of contrastive learning in text-video retrieval, focusing on the tension caused by modality gap and the noise introduced by false negatives. We show that such tension arises when gradients from negative pairs conflict with positive updates, restricting the optimization freedom of text anchors. To address this, we perform a first-order Taylor expansion of the InfoNCE loss and derive a pair-specific increment Δ_{ij} as an optimal adjustment direction within a trust region. By learning Δ_{ij} through a neural module conditioned on the semantic gap, and regularizing its structure, we enable more stable and interpretable optimization. Experiments on standard retrieval benchmarks confirm the effectiveness of this approach, and qualitative results demonstrate that Δ captures meaningful geometry for resolving representation conflicts.

References

- [1] Alexander A Alemi, Ian Fischer, Joshua V Dillon, and Kevin Murphy. Deep variational information bottleneck. *arXiv preprint arXiv:1612.00410*, 2016.
- [2] Lisa Anne Hendricks, Oliver Wang, Eli Shechtman, Josef Sivic, Trevor Darrell, and Bryan Russell. Localizing moments in video with natural language. In *Proceedings of the IEEE international conference on computer vision*, pages 5803–5812, 2017.
- [3] Alberto Baldrati, Marco Bertini, Tiberio Uricchio, and Alberto Del Bimbo. Conditioned and composed image retrieval combining and partially fine-tuning clip-based features. In *Proceedings of the IEEE/CVF Conference on Computer Vision and Pattern Recognition (CVPR) Workshops*, pages 4959–4968, June 2022.
- [4] Alberto Baldrati, Marco Bertini, Tiberio Uricchio, and Alberto Del Bimbo. Effective conditioned and composed image retrieval combining clip-based features. In *2022 IEEE/CVF Conference on Computer Vision and Pattern Recognition (CVPR)*, pages 21434–21442, 2022.
- [5] Simion-Vlad Bogolin, Ioana Croitoru, Hailin Jin, Yang Liu, and Samuel Albanie. Cross modal retrieval with querybank normalisation, 2022.
- [6] David Chen and William B Dolan. Collecting highly parallel data for paraphrase evaluation. In *Proceedings of the 49th annual meeting of the association for computational linguistics: human language technologies*, pages 190–200, 2011.
- [7] Tsai-Shien Chen, Wei-Chih Hung, Hung-Yu Tseng, Shao-Yi Chien, and Ming-Hsuan Yang. Incremental false negative detection for contrastive learning. *arXiv preprint arXiv:2106.03719*, 2021.
- [8] Xinlei Chen, Haoqi Fan, Ross Girshick, and Kaiming He. Improved baselines with momentum contrastive learning. *arXiv preprint arXiv:2003.04297*, 2020.
- [9] Xinlei Chen, Saining Xie, and Kaiming He. An empirical study of training self-supervised vision transformers. In *Proceedings of the IEEE/CVF international conference on computer vision*, pages 9640–9649, 2021.
- [10] Ching-Yao Chuang, Joshua Robinson, Yen-Chen Lin, Antonio Torralba, and Stefanie Jegelka. Debaised contrastive learning. *Advances in neural information processing systems*, 33:8765–8775, 2020.
- [11] Arthur P Dempster, Nan M Laird, and Donald B Rubin. Maximum likelihood from incomplete data via the em algorithm. *Journal of the royal statistical society: series B (methodological)*, 39(1):1–22, 1977.
- [12] Kingma Diederik. Adam: A method for stochastic optimization. (*No Title*), 2014.
- [13] Jianfeng Dong, Xianke Chen, Minsong Zhang, Xun Yang, Shujie Chen, Xirong Li, and Xun Wang. Partially relevant video retrieval. In *Proceedings of the 30th ACM International Conference on Multimedia*, MM ’22, page 246–257. ACM, October 2022.
- [14] Bo Fang, Wenhao Wu, Chang Liu, Yu Zhou, Yuxin Song, Weiping Wang, Xiangbo Shu, Xiangyang Ji, and Jingdong Wang. Uatvr: Uncertainty-adaptive text-video retrieval. In *Proceedings of the IEEE/CVF International Conference on Computer Vision*, pages 13723–13733, 2023.
- [15] Satya Krishna Gorti, Noël Vouitsis, Junwei Ma, Keyvan Golestan, Maksims Volkovs, Animesh Garg, and Guangwei Yu. X-pool: Cross-modal language-video attention for text-video retrieval. In *Proceedings of the IEEE/CVF conference on computer vision and pattern recognition*, pages 5006–5015, 2022.
- [16] Bo He, Jun Wang, Jieliu Qiu, Trung Bui, Abhinav Shrivastava, and Zhaowen Wang. Align and attend: Multimodal summarization with dual contrastive losses, 2023.
- [17] Kaiming He, Haoqi Fan, Yuxin Wu, Saining Xie, and Ross Girshick. Momentum contrast for unsupervised visual representation learning. In *Proceedings of the IEEE/CVF conference on computer vision and pattern recognition*, pages 9729–9738, 2020.

- [18] R Devon Hjelm, Alex Fedorov, Samuel Lavoie-Marchildon, Karan Grewal, Phil Bachman, Adam Trischler, and Yoshua Bengio. Learning deep representations by mutual information estimation and maximization. *arXiv preprint arXiv:1808.06670*, 2018.
- [19] Peng Jin, Jinfa Huang, Fenglin Liu, Xian Wu, Shen Ge, Guoli Song, David Clifton, and Jie Chen. Expectation-maximization contrastive learning for compact video-and-language representations. *Advances in neural information processing systems*, 35:30291–30306, 2022.
- [20] Peng Jin, Jinfa Huang, Pengfei Xiong, Shangxuan Tian, Chang Liu, Xiangyang Ji, Li Yuan, and Jie Chen. Video-text as game players: Hierarchical banzhaf interaction for cross-modal representation learning. In *Proceedings of the IEEE/CVF Conference on Computer Vision and Pattern Recognition*, pages 2472–2482, 2023.
- [21] Peng Jin, Hao Li, Zesen Cheng, Jinfa Huang, Zhennan Wang, Li Yuan, Chang Liu, and Jie Chen. Text-video retrieval with disentangled conceptualization and set-to-set alignment. *arXiv preprint arXiv:2305.12218*, 2023.
- [22] Peng Jin, Hao Li, Zesen Cheng, Kehan Li, Xiangyang Ji, Chang Liu, Li Yuan, and Jie Chen. Diffusionret: Generative text-video retrieval with diffusion model. In *Proceedings of the IEEE/CVF international conference on computer vision*, pages 2470–2481, 2023.
- [23] Weike Jin, Zhou Zhao, Xiaochun Cao, Jieming Zhu, Xiuqiang He, and Yueting Zhuang. Adaptive spatio-temporal graph enhanced vision-language representation for video qa. *IEEE Transactions on Image Processing*, 30:5477–5489, 2021.
- [24] Ranjay Krishna, Kenji Hata, Frederic Ren, Li Fei-Fei, and Juan Carlos Niebles. Dense-captioning events in videos. In *Proceedings of the IEEE international conference on computer vision*, pages 706–715, 2017.
- [25] Kuang-Huei Lee, Xi Chen, Gang Hua, Houdong Hu, and Xiaodong He. Stacked cross attention for image-text matching. In *Proceedings of the European Conference on Computer Vision (ECCV)*, September 2018.
- [26] Pandeng Li, Chen-Wei Xie, Liming Zhao, Hongtao Xie, Jiannan Ge, Yun Zheng, Deli Zhao, and Yongdong Zhang. Progressive spatio-temporal prototype matching for text-video retrieval. In *Proceedings of the IEEE/CVF International Conference on Computer Vision*, pages 4100–4110, 2023.
- [27] Victor Weixin Liang, Yuhui Zhang, Yongchan Kwon, Serena Yeung, and James Y Zou. Mind the gap: Understanding the modality gap in multi-modal contrastive representation learning. *Advances in Neural Information Processing Systems*, 35:17612–17625, 2022.
- [28] Yuqi Liu, Pengfei Xiong, Luhui Xu, Shengming Cao, and Qin Jin. Ts2-net: Token shift and selection transformer for text-video retrieval. In *European conference on computer vision*, pages 319–335. Springer, 2022.
- [29] Huaishao Luo, Lei Ji, Ming Zhong, Yang Chen, Wen Lei, Nan Duan, and Tianrui Li. Clip4clip: An empirical study of clip for end to end video clip retrieval and captioning. *Neurocomputing*, 508:293–304, 2022.
- [30] Yiwei Ma, Guohai Xu, Xiaoshuai Sun, Ming Yan, Ji Zhang, and Rongrong Ji. X-clip: End-to-end multi-grained contrastive learning for video-text retrieval, 2022.
- [31] Antoine Miech, Jean-Baptiste Alayrac, Lucas Smaira, Ivan Laptev, Josef Sivic, and Andrew Zisserman. End-to-end learning of visual representations from uncurated instructional videos, 2020.
- [32] Aaron van den Oord, Yazhe Li, and Oriol Vinyals. Representation learning with contrastive predictive coding. *arXiv preprint arXiv:1807.03748*, 2018.
- [33] Alec Radford, Jong Wook Kim, Chris Hallacy, Aditya Ramesh, Gabriel Goh, Sandhini Agarwal, Girish Sastry, Amanda Askell, Pamela Mishkin, Jack Clark, et al. Learning transferable visual models from natural language supervision. In *International conference on machine learning*, pages 8748–8763. PMLR, 2021.
- [34] Kaibin Tian, Yanhua Cheng, Yi Liu, Xinglin Hou, Quan Chen, and Han Li. Towards efficient and effective text-to-video retrieval with coarse-to-fine visual representation learning. In *Proceedings of the AAAI Conference on Artificial Intelligence*, volume 38, pages 5207–5214, 2024.
- [35] Naftali Tishby, Fernando C Pereira, and William Bialek. The information bottleneck method. *arXiv preprint physics/0004057*, 2000.
- [36] Ashish Vaswani, Noam Shazeer, Niki Parmar, Jakob Uszkoreit, Llion Jones, Aidan N Gomez, Łukasz Kaiser, and Illia Polosukhin. Attention is all you need. *Advances in neural information processing systems*, 30, 2017.
- [37] Bairui Wang, Lin Ma, Wei Zhang, and Wei Liu. Reconstruction network for video captioning. In *Proceedings of the IEEE Conference on Computer Vision and Pattern Recognition (CVPR)*, June 2018.

- [38] Feng Wang and Huaping Liu. Understanding the behaviour of contrastive loss. In *Proceedings of the IEEE/CVF conference on computer vision and pattern recognition*, pages 2495–2504, 2021.
- [39] Qiang Wang, Yanhao Zhang, Yun Zheng, Pan Pan, and Xian-Sheng Hua. Disentangled representation learning for text-video retrieval. *arXiv:2203.07111*, 2022.
- [40] Tongzhou Wang and Phillip Isola. Understanding contrastive representation learning through alignment and uniformity on the hypersphere. In *International conference on machine learning*, pages 9929–9939. PMLR, 2020.
- [41] Yimu Wang, Xiangru Jian, and Bo Xue. Balance act: Mitigating hubness in cross-modal retrieval with query and gallery banks, 2023.
- [42] Ziyang Wang, Yi-Lin Sung, Feng Cheng, Gedas Bertasius, and Mohit Bansal. Unified coarse-to-fine alignment for video-text retrieval, 2023.
- [43] Zhirong Wu, Yuanjun Xiong, Stella X Yu, and Dahua Lin. Unsupervised feature learning via non-parametric instance discrimination. In *Proceedings of the IEEE conference on computer vision and pattern recognition*, pages 3733–3742, 2018.
- [44] Hu Xu, Gargi Ghosh, Po-Yao Huang, Dmytro Okhonko, Armen Aghajanyan, Florian Metze, Luke Zettlemoyer, and Christoph Feichtenhofer. Videoclip: Contrastive pre-training for zero-shot video-text understanding, 2021.
- [45] Jun Xu, Tao Mei, Ting Yao, and Yong Rui. Msr-vtt: A large video description dataset for bridging video and language. In *Proceedings of the IEEE conference on computer vision and pattern recognition*, pages 5288–5296, 2016.
- [46] Xiangpeng Yang, Linchao Zhu, Xiaohan Wang, and Yi Yang. Dgl: Dynamic global-local prompt tuning for text-video retrieval, 2024.
- [47] Can Yaras, Siyi Chen, Peng Wang, and Qing Qu. Explaining and mitigating the modality gap in contrastive multimodal learning. *arXiv preprint arXiv:2412.07909*, 2024.
- [48] Youngjae Yu, Hyungjin Ko, Jongwook Choi, and Gunhee Kim. End-to-end concept word detection for video captioning, retrieval, and question answering. In *Proceedings of the IEEE conference on computer vision and pattern recognition*, pages 3165–3173, 2017.
- [49] Haonan Zhang, Pengpeng Zeng, Lianli Gao, Jingkuan Song, and Heng Tao Shen. Mpt: Multi-grained prompt tuning for text-video retrieval. In *Proceedings of the 32nd ACM International Conference on Multimedia*, pages 1206–1214, 2024.

A Limitations

While our method successfully reduces the tension between text and video embeddings by optimizing pair-wise Δ_{ij} based on the direction that minimizes the InfoNCE loss, several limitations remain:

A.1 Lack of Modality Alignment

The fundamental issue of modality gap persists. Despite reducing the tension between the embeddings of text and video, the two modalities still reside in completely disjoint regions of the representation space. Our method alleviates the modality gap by offloading some of the gradient tension, but it does not align the two modalities in a meaningful way. The solution we propose does not explicitly enforce a shared representation space between text and video; rather, it reduces the gradient tension through the optimization of Δ_{ij} . As a result, the method mitigates the effects of the modality gap and reduces some noise, but it does not address the root cause of the misalignment between the two modalities.

A.2 Lack of Generalized Supervision for Δ

Our approach relies heavily on adjusting Δ_{ij} through gradient-based optimization, but Δ_{ij} lacks a more generalizable supervision signal. Currently, we are optimizing each pair-wise Δ_{ij} based solely on the gradient of the InfoNCE loss, which only loosely guides the optimization direction. While this helps alleviate the tension between positive and negative pairs, it does not provide a stronger supervisory signal to guide the model toward a better generalization across unseen data.

In summary, while the method presents an effective way of mitigating gradient tension and improving the performance of contrastive learning, these limitations highlight areas for further development in future work.

B More Ablation Experiments

In the next four experiments conducted on the MSR-VTT-1KA dataset, we investigated the impact of different combinations of c and η , the impact of the scale coefficient σ in the directional diversity regularization, the impact of the lower bound of Norm-Based Regularization of Trust-Region Radii and the impact of the anchor choice of \mathcal{L}_{IB} .

B.1 Combination of Context Modality type c and η Choices

As shown in Table 4, the results show: 1) Fine-tuning the text side is better: By comparing different configurations of c and η , fine-tuning the text side consistently outperforms other choices. Specifically, when $c = t_i$ and $\eta = 1$, the text representation adjusts the increment Δ effectively, allowing for a higher semantic distinction of the increment. 2) Choosing v as the context for ψ is better: In this experiment, choosing

the video modality v_j as the context for ψ yielded better results, especially when $c = v_j$ and $\eta = 1$, achieving the highest R@1 score. This suggests that learning more fine-grained representations from the video modality helps improve cross-modal interactions and boosts performance.

Since videos in the MSR-VTT dataset are often clips from the same source video, leading to a high number of similar video samples, fine-grained learning becomes crucial. Adding this fine-grained adjustment to the text side enables Δ to have better semantic distinction and enhances retrieval performance.

B.2 Ablation of the Regularization Scale Coefficient σ in Directional Diversity

As shown in Table 5, the results indicate: 1) Smaller σ (0.5): When σ is small, the diversity of the delta vectors is limited, which weakens the model’s ability to learn fine-

Table 4: Ablation on combinations of c and η (modality/context choice).

setting		R@1↑	R@5↑	R@10↑	MdR↓	MnR↓
$c = t_i$	$\eta = -1$	46.6	74.2	83.8	2.0	12.9
$c = t_i$	$\eta = +1$	48.2	74.2	83.2	2.0	12.9
$c = v_j$	$\eta = -1$	47.8	74.1	82.8	2.0	12.4
$c = v_j$	$\eta = +1$	49.1	74.7	83.6	2.0	12.0

grained representations. Although the R@1 score is 47.6, the model’s ability to distinguish between samples is reduced due to limited directional diversity. 2) Moderate σ (1.0 and 2.0): In these configurations, the directional diversity of delta vectors is more balanced, effectively enhancing the model’s ability to capture cross-modal variations. The R@1 score improves to 49.1, showing that appropriate variance increases retrieval performance. 3) Larger σ (3.0 and 5.0): When σ is too large, the directional difference between delta vectors becomes excessive, introducing noise and decreasing model performance. Specifically, with $\sigma = 3.0$, the R@1 score drops to 46.2.

From this experiment, it is evident that an appropriately moderate σ enables delta vectors to have useful directional diversity, thereby improving cross-modal representation learning. However, excessively large σ may result in noise that negatively impacts model performance.

Table 5: Ablation on scale coefficient σ for directional diversity.

σ	R@1↑	R@5↑	R@10↑	MdR↓	MnR↓
0.5	47.6	74.5	83.4	2.0	12.1
1.0	48.5	74.4	83.9	2.0	12.1
2.0	49.1	74.7	83.6	2.0	12.0
3.0	46.2	74.4	82.9	2.0	12.1
4.0	47.0	74.3	83.4	2.0	12.1
5.0	47.2	74.1	82.8	2.0	12.4

B.3 Ablation on Δ Norm Regularization Strength

We investigate the effect of varying the lower bound factor λ , which controls the target margin of ε separation within each anchor t_i . As shown in Figure 3, increasing λ from 0.1 to 0.5 improves R@1, with the best performance at $\lambda = 0.5$. This suggests that moderate diversity in ε_{ij} is beneficial for enhancing semantic discrimination. However, as λ increases further, performance degrades, likely due to over-regularization.

To mitigate the instability introduced by hard truncation (i.e., directly thresholding ε_{ij}), we also experiment with a smooth approximation using a log-sum-exp formulation:

$$\mathcal{L}_{\varepsilon-\text{LogSumExp}} = \log \left(1 + \frac{1}{B} \sum_{j=1}^B \exp \left(-(\varepsilon_{ij} - \bar{\varepsilon}_i)^2 \right) \right), \quad \bar{\varepsilon}_i = \frac{1}{B} \sum_{j=1}^B \varepsilon_{ij}$$

Although this variant imposes a natural lower bound and provides vanishing gradients near convergence, it does not significantly improve retrieval. We hypothesize that this is due to gradient saturation when the variance among ε_{ij} becomes too large, which in turn weakens the ability to further enforce directional separation. Unlike contrastive margins that encourage explicit pairwise gaps, the log-sum-exp loss lacks sufficient directional tension to align with the InfoNCE objective.

B.4 Effect of Anchor Choice in \mathcal{L}_{IB}

To examine the role of modality anchoring in the information bottleneck regularization, we compare two variants of the KL divergence loss \mathcal{L}_{IB} applied on the learned increments Δ_{ij} . In both cases, Δ_{ij} is modeled as a Gaussian variable, but we anchor its distribution either from the video side (i.e., conditionally modeling Δ given v_j) or the text side (t_i). Results are shown in Table 6.

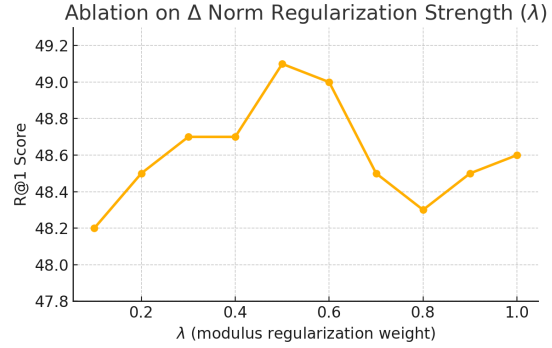


Figure 3: R@1 score with varying λ for Δ norm regularization.

Table 6: Effect of anchor choice in KL regularization \mathcal{L}_{IB} . Anchoring on v yields better performance.

Anchor	R@1	R@5	R@10	MedR	MnR
t_i (text)	47.9	74.9	83.8	2.0	12.5
v_j (video)	49.1	<u>74.7</u>	83.6	2.0	12.0

We observe that using the video as the anchor yields significantly better retrieval performance. This suggests that the information bottleneck not only suppresses unnecessary variance in Δ , but also

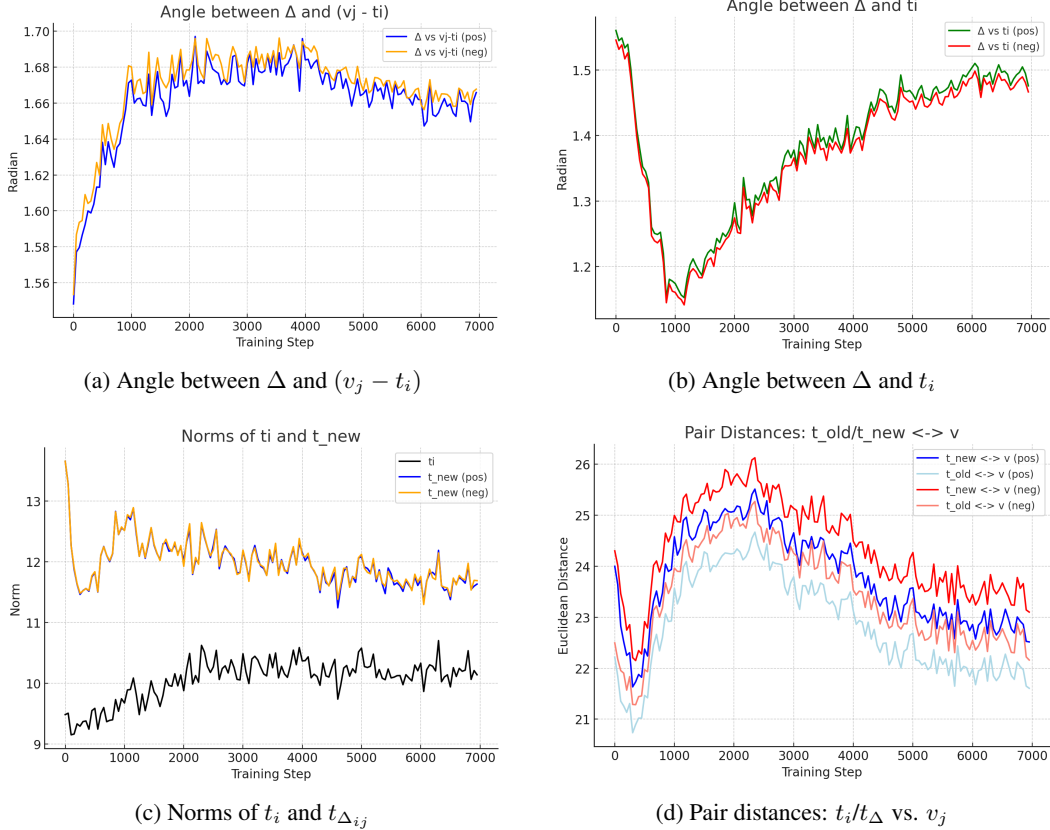


Figure 4: Training dynamics of the learned modality-gap vector Δ . t_{new} denotes t_{Δ} . (a) Δ grows increasingly orthogonal to the initial modality gap, indicating embedding space expansion. (b) Δ initially aligns with the anchor t_i , then deviates to encode semantic distinctions. (c) Updated embeddings t_{new} operate under larger norms, enlarging the contrastive space. (d) Pairwise distances increase and then stabilize, reflecting semantic separation and convergence.

guides the model to extract task-relevant signals from the noisier modality—videos in this case. Since Δ is generated based on the initial pairwise difference ($v_j - t_i$ or $t_i - v_j$), it inherently reflects the model’s prior on how to reconcile the cross-modal gap. Videos tend to carry more diverse and redundant visual information, and anchoring the KL constraint on v_j allows the model to compress this input through Δ , effectively learning a semantically meaningful adjustment. Conversely, anchoring on t_i fails to suppress visual redundancy, and the resulting Δ captures less structured or discriminative transformations, thereby degrading alignment quality. This analysis highlights that Δ acts not only as a tension offloader and false-negative noise suppressor, but also as a structured bottleneck pathway between text and video.

C Analysis of Δ Behavior During Training

To better understand the role and dynamics of the learned modality-gap vector Δ throughout training, we visualize four key aspects of Δ ’s behavior, presented in Figure A1 to A4. These analyses reveal the underlying geometric transformations and provide further insight into how Δ facilitates optimization under InfoNCE loss. We will continue conducting ablation studies on the Text-to-Video retrieval task using the MSR-VTT [45] dataset.

C.1 Angle between Δ and $(v_j - t_i)$

As shown in Figure 4a, we track the angle between Δ and the initial cross-modal gap vector $v_j - t_i$ throughout training, for both positive and negative pairs. At initialization, this angle is close to $\frac{\pi}{2}$,

indicating that Δ is nearly orthogonal to $v_j - t_i$, and thus carries no meaningful alignment with the cross-modal semantic gap. This implies that the early Δ vectors do not differentiate between positive and negative pairs, acting more like isotropic perturbations in space. As training proceeds, however, this angle gradually increases into the obtuse region for both positive and negative samples. This reflects a significant shift in behavior—rather than attempting to directly bridge the modality gap $v_j - t_i$, the model learns to push t_i away from v_j , effectively offloading the gradient tension induced by the modality gap and false negative interference. This offloading allows contrastive learning to take place in an expanded embedding space, where Δ modulates the representation geometry to ease the optimization burden. This trend is corroborated by Figure 4d, where the Euclidean distances between the updated text embeddings $t_{\Delta_{ij}} = t_i + \Delta_{ij}$ and v_j become significantly larger than the original distances $\|t_i - v_j\|$, for both positive and negative samples. That is, Δ introduces a global scaling effect in the representation space, and contrastive optimization is carried out under a larger geometric regime.

Interestingly, the new positive pair distances $\|t_{\Delta_{ii}} - v_i\|$ are also larger than their original counterparts $\|t_i - v_i\|$. Though this seems counterintuitive—since the gradient of InfoNCE with respect to Δ pushes toward v_i —it actually reflects the relative nature of the InfoNCE loss. The network does not aim to minimize absolute distances, but rather to increase the similarity margin between matched and mismatched pairs. Thus, pushing all embeddings outward in norm (as further validated in Figure 4c) gives the model more room to maneuver in angular space, while the cosine similarity objective remains stable under such rescaling. This aligns with our design intent: to leverage Δ as a structural carrier for modality-aware tension redistribution, providing optimization flexibility on a normalized manifold.

Moreover, in early training stages, the angles between Δ and $v_j - t_i$ are nearly identical for positive and negative samples, showing that the model has not yet learned to encode fine-grained pairwise differences. But as training advances, a slight but consistent gap emerges— Δ for positive samples tends to have slightly smaller angles than that of negatives. This subtle divergence signals that Δ has begun to capture semantically meaningful pair-level distinctions, enabling more discriminative alignment in later stages.

C.2 Angle between Δ and t_i

As shown in Figure 4b, the angle between Δ and t_i exhibits a distinct pattern: it decreases rapidly in the early training phase, indicating that Δ is initially aligned with the anchor text embedding. This suggests that the model’s default behavior is to trust the prior structure of the text space and apply similar Δ directions across different v_j , especially when pairwise semantic differences are not yet learned.

However, over time, this alignment loosens— Δ deviates further from t_i as the model begins to adapt to modality-specific differences. This marks a transition where the network ψ no longer treats the anchor t_i as a default direction and instead generates Δ based on nuanced distinctions across the visual features v_j , thus leading to more expressive and semantically grounded Δ vectors.

C.3 Pair Distances between Text and Video Features

Figure 4d visualizes the Euclidean distances between text and video pairs over the course of training, comparing both the original pairs $t_i \leftrightarrow v_j$ and the updated pairs $t_{\Delta_{ij}} \leftrightarrow v_j$, across positive and negative samples. Several important patterns emerge: First, we observe that positive pair distances remain consistently smaller than negative pair distances, both in the original and updated forms. This confirms that the learned Δ not only preserves the basic alignment structure of contrastive learning but also enhances semantic discrimination, effectively encoding fine-grained pairwise structure through the transformation. Second, for both positive and negative pairs, the distances between t_{Δ} and v are larger than those between the original t and v , demonstrating that the model pushes the updated text embeddings into a larger-scale embedding regime. This is precisely in line with our gradient tension offloading design: Δ introduces a controlled displacement that alleviates the direct optimization pressure on t_i , allowing contrastive comparisons to operate within a higher-norm, more expressive space, as also supported by Figure 4c. The evolution of the distance curves over time also reflects meaningful training dynamics. Initially, all distances decrease, which we interpret as a normalization phase — embedding distributions at initialization are noisy and unstructured, and the model first

compresses them into a tighter, more consistent geometric configuration. This is followed by a steady increase in distances, as the model begins to explicitly separate positive and negative samples to satisfy the InfoNCE objective. Finally, all curves converge and stabilize into a bounded range, suggesting that the semantic configuration of the embedding space has reached a relatively converged structural state.

Taken together, these observations highlight the critical role of Δ not only in scaling the embedding geometry but also in encoding structurally-aware, semantically-aligned displacements that facilitate tension redistribution and enable robust representation learning.

D Why We Don't Use an Initial $\Delta_{ij}^* = 0$ Expansion and the Need for a Non-Zero Initial Δ_{ij}^*

D.1 Introduction to the Issue

In the previous approach, we considered using multiple variables Δ_{ij} to distribute the gradient impact of each video v_j on the text embedding t_i . However, the specific form of Δ_{ij} was unclear. The idea was to update each Δ_{ij} in the direction that would reduce the InfoNCE loss. A natural first step was to expand the loss function \mathcal{L}_i as a Taylor expansion around the initial state $\Delta_{ij}^* = 0$, which would correspond to an expansion solely based on t_i .

However, this expansion introduces a key issue: the gradient terms in each Δ_{ij} expansion are computed assuming that all other Δ_{ik} are zero. This neglects the interactions between different Δ_{ij} and effectively decouples the updates for each pair. Since InfoNCE loss requires comparing relative similarities between different pairs, this decoupled approach violates the fundamental nature of the contrastive learning objective, as it does not respect the relative comparisons between the cosine similarities of different text-video pairs.

D.2 Why Expanding with $\Delta_{ij}^* = 0$ Is Inadequate

When $\Delta_{ij}^* = 0$ for all j , the gradient expansion for each pair Δ_{ij} looks like:

$$\mathcal{L}_i(\Delta_{ij}^*) \approx \mathcal{L}_i(0) + \sum_{j=1}^B [\nabla_{\Delta_{ij}} \mathcal{L}_i(0)]^\top \Delta_{ij}, \quad (17)$$

where $\nabla_{\Delta_{ij}} \mathcal{L}_i(0)$ is the gradient of the loss evaluated at $\Delta_{ij} = 0$. In this case, the gradient $p_{ij} - y_{ij}$ is computed as:

$$\nabla_{\Delta_{ij}} \mathcal{L}_i(0) = (p_{ij}(0) - y_{ij}) \nabla_{\Delta_{ij}} \cos_{ij}(0), \quad (18)$$

where $p_{ij}(0)$ is the softmax term evaluated at the cosine similarity $\cos(t_i, v_j)$. This expansion does not account for the interdependence between different Δ_{ik} , and the gradients are computed as if each Δ_{ij} were independent of all other Δ_{ik} , which violates the relative comparison required for contrastive learning.

D.3 The Need for a Non-Zero Initial Δ_{ij}^*

To avoid this issue, we recognize that each Δ_{ij} should be updated in a way that reflects the interdependence between different pairs, not just based on an independent text-video pair. The gradient of the InfoNCE loss must be evaluated with respect to the current state of all Δ_{ij} , not just the initial zero state.

Thus, we need to initialize Δ_{ij}^* in a way that reflects the current state of all other pairs rather than assuming they are zero. The update for each Δ_{ij} should respect the relationship between all the pairwise similarities, as the optimization of one pair affects the relative similarity between all other pairs.

In this case, the correct approach is to perform the first-order Taylor expansion around a non-zero state $\Delta_{ij}^{(t)}$ that has already been optimized for several steps. This allows us to incorporate the effect

of each pair Δ_{ij} on the entire set of pairwise comparisons, thus preserving the relative relationships that are critical for InfoNCE loss.

D.4 Optimization Objective and Trust-Region Constrained Solution

Having established the need for a coupled, non-zero initialization of Δ_{ij} to preserve the relative structure required by InfoNCE, we now formulate the optimization problem for finding the optimal update direction under a trust region constraint. Specifically, we assume a trust region radius ε that bounds the magnitude of each Δ_{ij} and analyze the solutions in both the single-step (non-iterative) and iterative update settings.

Non-Iterative First-Order Update We consider the first-order Taylor expansion of the per-anchor loss \mathcal{L}_i with respect to Δ_{ij} evaluated at the origin:

$$\mathcal{L}_i(\Delta_{ij}) \approx \mathcal{L}_i(0) + \nabla_{\Delta_{ij}} \mathcal{L}_i(0)^\top \cdot \Delta_{ij}, \quad (19)$$

subject to the trust-region constraint $\|\Delta_{ij}\| \leq \varepsilon$. This forms a standard constrained linear minimization problem, where the optimal Δ_{ij} minimizes the inner product with the gradient. By the Cauchy–Schwarz inequality:

$$\nabla_{\Delta_{ij}} \mathcal{L}_i^\top \cdot \Delta_{ij} \geq -\|\nabla_{\Delta_{ij}} \mathcal{L}_i\| \cdot \|\Delta_{ij}\|, \quad (20)$$

equality holds when Δ_{ij} and $-\nabla_{\Delta_{ij}} \mathcal{L}_i$ are colinear. Thus, the optimal update is in the steepest descent direction:

$$\Delta_{ij}^* = -\varepsilon \cdot \frac{\nabla_{\Delta_{ij}} \mathcal{L}_i}{\|\nabla_{\Delta_{ij}} \mathcal{L}_i\|}. \quad (21)$$

This solution, however, ignores the coupling between different Δ_{ik} and breaks the softmax structure, violating the relative comparison essential to InfoNCE, as discussed in the subsection above. Therefore, a more faithful solution must incorporate the influence of all Δ_{ij} jointly.

Iterative Update with Coupled Expansion We instead consider the Taylor expansion centered at the current state $\Delta_{ij}^{(t)}$, capturing the coupled contributions of all other $\Delta_{ik} \neq \Delta_{ij}$. We seek the next update step:

$$\Delta_{ij}^{(t+1)} = \Delta_{ij}^{(t)} + \delta, \quad \text{with } \|\Delta_{ij}^{(t+1)}\| \leq \varepsilon. \quad (22)$$

We again minimize the first-order approximation:

$$\mathcal{L}_i(\Delta_{ij}^{(t+1)}) \approx \mathcal{L}_i(\Delta_{ij}^{(t)}) + \nabla_{\Delta_{ij}} \mathcal{L}_i^{(t)\top} \cdot (\Delta_{ij}^{(t+1)} - \Delta_{ij}^{(t)}).$$

Letting $\hat{g}_{ij}^{(t)} = \nabla_{\Delta_{ij}} \mathcal{L}_i^{(t)} / \|\nabla_{\Delta_{ij}} \mathcal{L}_i^{(t)}\|$, we propose a step in the steepest descent direction:

$$\Delta_{ij}^{(t+1)} = \Delta_{ij}^{(t)} - \alpha_{ij}^{(t)} \cdot \hat{g}_{ij}^{(t)}. \quad (23)$$

To satisfy the norm constraint $\|\Delta_{ij}^{(t+1)}\| \leq \varepsilon$, we solve for the maximum allowable step size $\alpha_{ij}^{(t)}$ using the triangle and Cauchy–Schwarz inequalities:

$$\|\Delta_{ij}^{(t)} - \alpha_{ij}^{(t)} \hat{g}_{ij}^{(t)}\|^2 \leq \varepsilon^2. \quad (24)$$

Expanding this yields the quadratic inequality:

$$\alpha_{ij}^{(t)2} - 2\alpha_{ij}^{(t)} \Delta_{ij}^{(t)\top} \hat{g}_{ij}^{(t)} + \|\Delta_{ij}^{(t)}\|^2 - \varepsilon^2 \leq 0, \quad (25)$$

whose maximal feasible solution is:

$$\alpha_{ij}^{(t)} = \Delta_{ij}^{(t)\top} \hat{g}_{ij}^{(t)} + \sqrt{\left(\Delta_{ij}^{(t)\top} \hat{g}_{ij}^{(t)}\right)^2 - \|\Delta_{ij}^{(t)}\|^2 + \varepsilon^2}. \quad (26)$$

Thus, the update maintains the trust region while moving in the steepest descent direction under the coupled loss landscape.

D.5 Why Use Neural Networks for Approximation?

The reason we opt for neural networks to approximate the current state of Δ_{ij} rather than directly solving for each Δ_{ij} through numerical optimization is primarily due to efficiency and scalability:

Handling Non-Linearities: The relationship between the embeddings of text and video is highly non-linear. Neural networks are particularly well-suited for learning such complex, non-linear mappings, allowing the model to effectively learn the best updates for Δ_{ij} without requiring explicit mathematical formulations for each pairwise interaction.

Scalability: As the size of the dataset increases, the computational cost of directly solving each Δ_{ij} grows rapidly. Neural networks allow for scalable learning since once trained, they can quickly compute updates for large batches without re-solving the optimization problem for each individual pair, making them a more practical choice in real-world settings.

In short, neural networks allow for faster convergence and better scalability compared to direct numerical solutions, making them essential for large-scale contrastive learning tasks.

E Computational Complexity Analysis.

In our proposed GARE framework, each mini-batch of size B involves the prediction of a pair-specific increment $\Delta_{ij} \in \mathbb{R}^D$ for all text-video pairs. This yields a forward computational complexity of $\mathcal{O}(B^2D)$, since the learned increment network ψ generates $B \times B$ outputs of dimension D . While quadratic in batch size, this cost is efficiently amortized during training and can be parallelized on modern hardware.

Importantly, this design avoids the substantial overhead required by a numerical optimization scheme. If one were to directly minimize the first-order Taylor expansion of the loss with respect to Δ using explicit iterative updates, two key obstacles arise: (1) The expansion is strictly first-order and lacks nonlinear modeling capacity, making it poorly suited for generalizing to unseen test-time structures; (2) Due to the softmax-coupled nature of InfoNCE, the gradients of each Δ_{ij} are entangled with all other Δ_{ik} , requiring T rounds of joint optimization for a converged update. As a result, the overall complexity escalates to $\mathcal{O}(TB^2D)$, where T denotes the number of inner optimization steps. In addition to the increased cost, this setup suffers from severe gradient coupling and lacks a principled way to impose per-pair trust region constraints such as $|\Delta_{ij}| \leq \varepsilon$.

By contrast, our network-based approach amortizes this optimization and learns to implicitly enforce structure-aware constraints via training, making it not only more efficient but also more generalizable.